

Quantitative MR imaging of ex vivo intracranial atherosclerotic plaques at 7.0 tesla

A.A. Harteveld¹, N.P. Denswil², J.C.W. Siero¹, J.J.M. Zwanenburg^{1,3}, A. Vink⁴, W.G.M. Spliet⁴, P.R. Luijten¹, M.J. Daemen², J. Hendrikse¹, and A.G. van der Kolk¹
¹Department of Radiology, University Medical Center Utrecht, Utrecht, Netherlands, ²Department of Pathology, Academic Medical Center, Amsterdam, Netherlands, ³Image Sciences Institute, University Medical Center Utrecht, Utrecht, Netherlands, ⁴Department of Pathology, University Medical Center Utrecht, Utrecht, Netherlands

Introduction: Intracranial atherosclerosis is one of the main causes of ischemic stroke and transient ischemic attack (TIA)¹. In recent years, several intracranial vessel wall imaging techniques using (ultra)high-field magnetic resonance imaging (MRI) have emerged for the evaluation and characterization of atherosclerotic vessel wall lesions *in vivo*. However, a thorough validation of MRI results of intracranial plaques with histopathology is still lacking^{2,3}. As a consequence, we do not know to what extent intracranial plaque contrast differences seen with these high field strengths represent different plaque components, like they do in carotid artery atherosclerotic plaques. The purpose of this study was to validate the signal characteristics of different intracranial plaque components with *quantitative* MRI at 7 tesla (7T). Quantitative MR measurements have the potential to provide specific information of the NMR tissue properties of different atherosclerotic plaque components, therefore allowing a quantitative differentiation between these components.

Methods: Fifteen anonymous circle of Willis (CoW) specimens with a high atherosclerotic plaque burden were selected for this study. The specimens included the major arteries of the CoW. All specimens were cleaned from clotted blood products and embedded in a petri dish containing 2% agarose solution. Cactus spines were used as fiducials and placed at 15 locations to enable spatial correlation with histology⁴. The embedded specimens were scanned on a 7T whole body system (Philips Healthcare), with a custom-made 16-channel dedicated surface coil (MR Coils BV), and a volume transmit/receive coil for transmission (Nova Medical). A scan protocol containing sequences with different contrast weightings was used to image the specimens, from which quantitative MR parameter maps were calculated. To obtain the quantitative T₁, T₂ and PD maps, acquisition was performed at two specific flip angles according to the DESPOT1 and DESPOT2 method⁵. T₂* maps were obtained using a dual-echo 3D T₂*-weighted scan. The following scan parameters were used: DESPOT1 sequence, field-of-view (FOV) 150x150x19.9mm³, acquired resolution 0.13x0.13x0.13mm³, TR/TE 26/4.3ms, flip angles (FA) 11 and 44 degrees, matrix size 1152x1154, bandwidth (BW) 165.1 Hz/pixel, 4 repeated scans, TFE factor 1154; DESPOT2 sequence, FOV 150x150x19.9mm³, acquired resolution 0.13x0.13x0.13mm³, TR/TE 36/18ms, FA 12 and 62 degrees, matrix size 1152x1152, BW 40.5 Hz/pixel, 3 dynamic scans, TFE factor 1152; T₂* map sequence, FOV 150x150x19.9mm³, acquired resolution 0.13x0.13x0.13mm³, TR/TE1/TE2 53/6.2/25.7ms, FA 29 degrees, matrix size 1152x1154, BW 101.3 Hz/pixel, NSA 1, TFE factor 1154. Total scan time was approximately 19h45min. To mitigate potential artifacts caused by scanner frequency drift, the scanner resonance frequency was measured and adjusted between each shot. B1 correction was performed during calculation of the parametric maps, to correct for B1 inhomogeneity within the specimen. After imaging, samples were taken from the marked locations for histological evaluation. Classification of the histological slides was performed according to the modified American Heart Association classification by Virmani et al.⁶ For analysis of different plaque components, only plaques scored as advanced – therefore including several components – were used. Based on the identified plaque components (lipid accumulation, fibrous tissue, fibrous cap, and calcifications) in a histological slide, regions of interest (ROIs) were drawn within the corresponding regions on the original T₁-weighted DESPOT1 images and used to calculate the mean T₁, T₂, PD and T₂* values for those regions in the MR parameter maps. Since the assumption of homogeneity of variance was not met, Welch's test was conducted to compare the mean ROI values of the different tissue components. Games-Howell's post hoc tests were performed for pairwise comparisons.

Results: MRI and histopathology of 36 different cross sections of advanced atherosclerotic plaques were matched and used for the ROI analysis. In Figure 1 an example is given of one matched cross section. Table 1 shows the mean T₁, T₂, PD and T₂* values for the identified tissue components. Mean T₁, T₂, PD and T₂* were significantly different between the different tissue components (T₁: F(4,38)=59.19, p<.001; PD: F(4,90)=37.10, p<.001; T₂: F(4,24)=11.97, p<.001; T₂*: F(4,26)=8.99, p<.001). Post hoc comparisons indicated the mean T₁ relaxation time of lipid accumulation (T₁=747 ± 156ms) was significantly different from fibrous cap (T₁=508 ± 121ms) and vessel wall (T₁=474 ± 158ms); fibrous tissue T₁ (T₁=663 ± 233ms) was also significantly different from vessel wall T₁. The mean T₂ relaxation times of both vessel wall (T₂=10 ± 4.0ms) and calcifications (T₂=9.2 ± 2.9ms) were significantly different from lipid accumulation (T₂=21 ± 7.1ms) and the fibrous tissue (T₂=18 ± 9.2ms). Calcifications were significantly different from all other identified tissue components for the T₁ and T₂* relaxation times, as well as the PD values.

Discussion: The presented ultrahigh-resolution MR imaging protocol shows that different atherosclerotic plaque components can be identified and characterized using multi-parametric quantitative T₁, T₂, T₂* and PD images of the intracranial arteries in *ex vivo* CoW specimen at 7T. For accurate measurement of the T₂(*) of the calcifications the SNR was probably too low. The next step is to make the translation to *in vivo* intracranial vessel wall MR imaging by developing sequences based on the NMR tissue properties of the identified atherosclerotic plaque components. This may eventually result in a dedicated MRI protocol for *in vivo* imaging of different intracranial plaque components.

References: ¹Arenillas JF, Stroke 2011; ²Kim JM, et al. Arch Neurol 2012; ³Qiao Y, et al. J Magn Reson Imaging 2011; ⁴Van der Kolk, et al. AJNR 2014, in press; ⁵Deoni SCL, et al. Magn Reson Med 2003; ⁶Virmani R, Arterioscler Thromb Vasc Biol 2000.

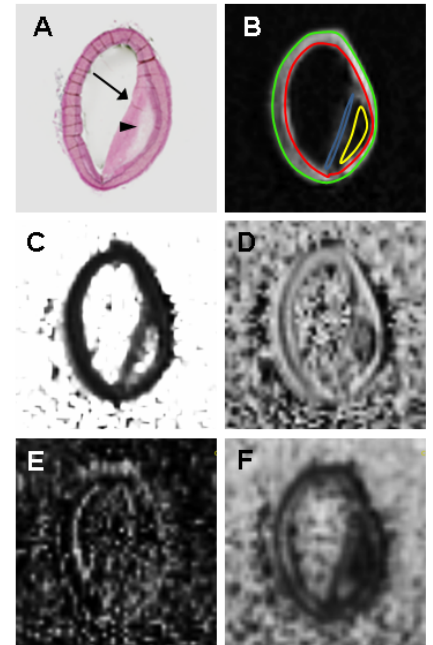


Figure 1. (A) Histological slide (HE staining) of a sample from one of the CoW specimen (left vertebral artery), with the corresponding original T1w image (B) and the calculated parametric maps: T₁ (C), PD (D), T₂ (E), and T₂* (F). (B) Regions of interest (ROIs) were drawn at the location of different tissue components identified in the histological slide to calculate the mean T₁-, T₂-, T₂*- and PD-values for those regions (yellow ROI: lipid accumulation; blue ROI: fibrous cap; green+red ROI: vessel wall). Arrow: thickened intima with atherosclerotic plaque; arrowhead: lipid accumulation within the plaque.

Table 1. NMR characteristics of different intracranial plaque tissue components (mean ± SD)

	Lipid accumulation (n=19)	Fibrous tissue (n=20)	Fibrous cap (n=15)	Calcifications (n=5)	Vessel wall (n=36)	p-value ^a
T ₁ (ms)	747 ± 156	663 ± 233	508 ± 121	262 ± 29	474 ± 158	<.001 [*]
T ₂ (ms)	21 ± 7.1	18 ± 9.2	15 ± 9.9	9.2 ± 2.9	10 ± 4.0	<.001 [*]
T ₂ * (ms)	18 ± 3.9	22 ± 9.4	22 ± 9.6	11 ± 2.8	18 ± 5.7	<.001 [*]
PD ^b	0.98 ± 0.14	1.09 ± 0.26	1.14 ± 0.20	0.19 ± 0.09	1.0 ± 0	<.001 [*]

^{*} P<0.05; ^aGroup differences were tested with Welch's test; ^bNormalized to vessel wall